

Water-Vapor Plasma-Based Surface Activation for Trichlorosilane Modification of PMMA

Timothy M. Long,^{†,‡,§,£} Shaurya Prakash,^{†,‡,£} Mark A. Shannon,^{*,†,‡,£} and Jeffrey S. Moore^{*,†,‡,§}

Beckman Institute for Advanced Science and Technology, University of Illinois at Urbana–Champaign, Urbana, Illinois 61801, Center for Nano-Scale Chemical-Electrical-Mechanical Manufacturing Systems (Nano-CEMMS), University of Illinois at Urbana–Champaign, Urbana, Illinois 61801, Department of Chemistry, University of Illinois at Urbana–Champaign, Urbana, Illinois 61801, and Department of Mechanical and Industrial Engineering, University of Illinois at Urbana–Champaign, Urbana, Illinois 61801

Received November 5, 2005. In Final Form: February 1, 2006

Separation rates and resolutions within capillary electrophoretic (CE) systems can be enhanced when surface ζ potentials are uniform with minimum deviations from ideal pluglike flow. Microfluidic CE devices based on poly(methyl methacrylate) (PMMA) are being developed due to the optical clarity, availability, stability, and reproducible electroosmotic flow (EOF) rates displayed by this polymer. Control of EOF in polymer-based CE systems can be achieved by surface ζ potential alteration through chemical modification. Herein, a method will be presented for the surface functionalization of PMMA with chemistry analogous to formation of trichlorosilane self-assembled monolayers on SiO₂. The current method involves two separate steps. First, surface activation with water-vapor plasma introduces surface hydroxylation. Second, treatment of the plasma-treated PMMA with a substituted trichlorosilane solution forms the functional surface layer. The modified surfaces were characterized using several analytical techniques, including water contact angle, X-ray photoelectron spectroscopy, Fourier transform infrared-attenuated total reflection, secondary ion mass spectroscopy, and measurement of EOF velocities within PMMA microchannels.

Introduction

Microelectromechanical systems (MEMS) offer the opportunity to miniaturize many common analytical techniques such as gas chromatography¹ or capillary electrophoretic² (CE) μ TAS (micro total-analytical-systems) for the rapid detection or analysis of minute sample quantities. Rapid throughput screening has become increasingly important for the environmental detection of chemical³ and biological⁴ warfare threats, as well as biological assays of DNA⁵ and proteins⁶ in chemical microreactors.⁷ While the application of MEMS fabrication technologies and miniaturization in silicon- and glass-based microdevices has been well-established,⁸ development of plastic-based devices offers an opportunity for rapid prototyping through traditional polymer

processing methods such as hot embossing⁹ and injection molding.¹⁰ The advantages offered by plastic microdevices in terms of lower cost, optical clarity, ease of fabrication, and availability have encouraged the development of these devices in substrates such as poly(dimethylsiloxane) (PDMS),¹¹ poly(methyl methacrylate) (PMMA),¹² Zeonor (a hydrocarbon cycloolefin polymer),¹³ poly(ethylene terephthalate) (PET),¹⁴ and poly(tetrafluoroethylene) (PTFE).¹⁵ Among these, PDMS has been the most popular due to its early introduction, as well as its nontoxicity and ready availability. For separation-based applications, PDMS has limitations due to inconsistent surface properties¹⁶ between devices, as well as leaching of low-molecular-weight oligomers from the bulk.¹⁷ The authors decided to focus on PMMA as a substrate for the assembly of polymer-based capillary electrophoresis due to its optical clarity, availability, stability to higher temperature (>100 °C) processing conditions, long-term stability, and reproducible electroosmotic flow rates.¹⁸

* To whom correspondence should be addressed. E-mail: moore@scs.uiuc.edu (J.S.M.); mshannon@uiuc.edu (M.A.S.).

[†] Beckman Institute for Advanced Science and Technology.

[‡] Center for Nano-Scale Chemical-Electrical-Mechanical Manufacturing Systems.

[§] Department of Chemistry.

[£] Department of Mechanical and Industrial Engineering.

(1) (a) Crume, C. *Environ. Test. Anal.* **2001**, *10*, 22–24. (b) Lindner, D. *Lab Chip* **2001**, *1*, 15N–19N.

(2) (a) Stachowiak, T. B.; Svec, F.; Frechet, J. M. J. *J. Chromatogr. A* **2004**, *1044*, 97–111. (b) Eeltink, S.; Roxing, G. P.; Koh, W. T. *Electrophoresis* **2003**, *24*, 3935–3961. (c) Bousse, L.; Cohen, C.; Nikiforov, T.; Chow, A.; Kopf-Sill, A. R.; Dubrow, R.; Parce, J. W. *Annu. Rev. Biophys. Biomol. Struct.* **2000**, *29*, 155–181.

(3) Lavrik, N. V.; Sepaniak, M. J.; Datskos, P. G. *Rev. Sci. Instr.* **2004**, *75*, 2229–2253.

(4) Bashir, R. *Adv. Drug Delivery Rev.* **2004**, *56*, 1565–1586.

(5) Chung, Y.-C.; Jan, M.-S.; Lin, Y.-C.; Lin, J.-H.; Cheng, W.-C.; Fan, C.-Y. *Lab Chip* **2004**, *4*, 141–147.

(6) Kato, M.; Gyoten, Y.; Sakai-Kato, K.; Nakajima, T.; Toyo'ok, T. *Anal. Chem.* **2004**, *76*, 6792–6796.

(7) Qu, H.; Wang, H.; Huang, Y.; Zhong, W.; Lu, H.; Kong, J.; Yang, P.; Liu, B. *Anal. Chem.* **2004**, *76*, 6426–6433.

(8) (a) Harrison, D. J.; Manz, J. A.; Fan, Z.; Ludi, H.; Widmers, H. M. *Anal. Chem.* **1992**, *64*, 1928–1932. (b) Woolley, A. T.; Mathies, R. A. *Proc. Natl. Acad. Sci.* **1994**, *91*, 11348–11352. (c) Jacobson, S. C.; Hergenroder, R.; Koutny, L. B.; Ramsey, J. M. *Anal. Chem.* **1994**, *66*, 1114–1118.

(9) Geissler, M.; Xia, Y. *Adv. Mater.* **2004**, *16*, 1249–1269.

(10) McCormick, R. M.; Nelson, R. J.; Alonso-Amigo, M. G.; Benvegna, D. J.; Hooper, H. H. *Anal. Chem.* **1997**, *69*, 2626–2630.

(11) McDonald, J. C.; Duffy, D. C.; Anderson, J. R.; Chiu, D. T.; Wu, H.; Schueller, O. J.; Whitesides, G. M. *Electrophoresis* **2000**, *21*, 27–40.

(12) Wang, Y.; Vaidya, B.; Farquar, H. D.; Stryjewski, W.; Hammer, R. P.; McCarley, R. L.; Soper, S. A.; Cheng, Y.-W.; Barany, F. *Anal. Chem.* **2003**, *75*, 1130–1140.

(13) (a) Kameoka, J.; Craighead, H. G.; Zhang, H.; Henion, J. *Anal. Chem.* **2001**, *73*, 1935–1941. (b) Tan, A.; Benetton, S.; Henion, J. D. *Anal. Chem.* **2003**, *75*, 5504–5511.

(14) Malmstadt, N.; Yager, P.; Hoffman, A. S.; Stayton, P. S. *Anal. Chem.* **2003**, *75*, 2943–2949.

(15) Lee, L. P.; Berger, S. A.; Liepmann, D.; Pruitt, L. *Sens. Actuators, A* **1998**, *71*, 144–149.

(16) (a) Wang, B.; Kanji, Z. A.; Dodwell, E.; Horton, J. H.; Oleschuk, R. D. *Electrophoresis* **2003**, *24*, 1442–1450. (b) Ng, J. M. K.; Gitlin, I.; Stroock, A. D.; Whitesides, G. M. *Electrophoresis* **2002**, *23*, 3461–3473.

(17) Hillborg, H.; Gedde, U. W. *Polymer* **1998**, *39*, 1991–1998.

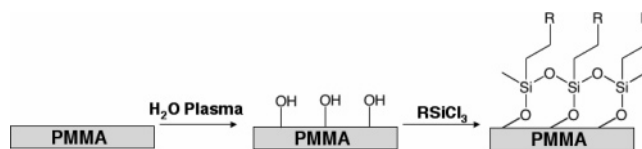
(18) Martynova, L.; Locascio, L. E.; Gaitan, M.; Kramer, G. W.; Christensen, R. G.; MacCrehan, W. A. *Anal. Chem.* **1997**, *69*, 4783–4789.

For CE applications, the separation rate and resolution can be enhanced by controlling the surface potentials within the microfluidic channels and making them as uniform as possible to assist in minimizing pressure-driven flows and subsequent deviation from pluglike flows.¹⁹ However, controlling the rate and direction of electroosmosis for polymer-based CE systems by altering the surface ζ potential through chemical modifications can be problematic compared to glass CE systems. Unlike the robust background of research on self-assembled monolayers (SAMs) on silicon and glass,²⁰ there have been limited examples of surface functionalization of polymers, PMMA in particular.

PMMA presents a surface of primarily methyl ester groups,²¹ limiting the standard chemical modification schemes that can be employed. Schemes to modify PMMA surfaces fall in two basic categories: photophysical and photochemical methods, such as laser alteration²² or UV irradiation in air,²³ and "wet" chemical modifications. One wet-chemical method relies on reduction of the ester groups to alcohols with lithium aluminum hydride in ether.²⁴ Alternatively, amino functionalities may be placed on the surface through aminolysis of the ester groups by treatment with a solution of *N*-lithiodiaminopropane in cyclohexane; this aminated surface could then be reacted with a substituted isocyanate.²⁵

Other chemical modification schemes involve plasma treatment of PMMA to activate the surface toward further reactions. Many different types of gas-plasmas have been cited in the literature including air,²⁶ oxygen,²⁷ UV-ozone,²⁸ H₂O,^{29–34} ammonia,³⁵ and argon³⁶ for modification of polymer surfaces. Plasma modification processes generate new chemical species on the surface of PMMA due to chemical reactions and physical sputtering (such as with Ar plasma) with active gas-phase species. These new chemical species can provide an anchor for attaching a series of different molecules that display different properties from the underlying bulk polymer. Use of oxygen plasmas has been the most common plasma treatment used for activation of PMMA surfaces. However, oxygen plasmas can lead to surface chain scission, cross-linking, or oxidation, generating oxidized functionalities ($-\text{CO}_x$, $-\text{OOH}$, and $-\text{C}=\text{O}$) on the surface.³⁷ In fact, peroxides generated on polymer surfaces have been utilized

Scheme 1. Two-Step Sequential Method Depicting Functionalization of PMMA Surfaces with a Trichlorosilane. The Method is Analogous to Formation of Silane Monolayers on SiO₂



for radical-based graft-polymerization of methacrylates and acrylamides.³⁸ UV-ozone treatment of PMMA in combination with methacryloylpropyltrimethoxysilane has been used for polymerization of polyacrylamide hydrogel plugs within microfluidic channels.³⁹ Argon and oxygen plasmas have also been shown to participate in surface sputtering in addition to modification, resulting in the physical removal of material from the surface.⁴⁰

Water-vapor plasma is a promising technology in contrast to oxygen plasma treatments. First, the water-vapor plasma generates high concentrations of reactive, excited water molecules and hydroxyl ($\cdot\text{OH}$) radicals in the gas-phase, increasing the likelihood of a densely hydroxylated surface.⁴¹ These concentrations of $\cdot\text{OH}$ radicals and excited water molecules lead to preferential hydroxylation of the surface with respect to oxidation.⁴² Second, due to lower levels of oxidized surface oligomers, hydrophobic recovery is slower.⁴³ Water-vapor plasma modification has also been carried out for many other polymers such as polyimide, polyethylene, polypropylene, polystyrene, polyoxymethylene, PET, and silicone rubber (SR) indicating the wide range of materials that can be hydroxyl-terminated with this plasma treatment.^{32–34} It has been previously shown that the primary functional moiety introduced by water-vapor plasma onto polymer surfaces, including PMMA, is the $-\text{OH}$ group.⁴⁴ The hydroxyl functional group is an important species because of its high chemical reactivity with respect to surface esters and it also increases hydrophilicity.

This paper describes a method for the surface functionalization of PMMA with chemistry analogous to formation of trichlorosilane SAMs on SiO₂. This method of surface functionalization relies on two sequential steps: surface activation with water-vapor plasma followed by modification reactions with a trichlorosilane (Scheme 1). Water-vapor plasma exposure introduces surface hydroxyls that react with a trichlorosilane, analogous to the surface reaction of silanol groups on silica (SiO₂) surfaces. The nature of these modified surfaces was surveyed utilizing contact angle data to show changes in wetting properties, X-ray photoelectron spectroscopy (XPS), Fourier transform infrared-attenuated total reflection (FTIR-ATR), and secondary ion mass spectroscopy (SIMS). To understand how these modifications influence the behavior of the channel wall on electroosmosis, electroosmotic flow (EOF) rates were measured in PMMA microfluidic devices and compared to untreated control PMMA devices. Further, nucleophilic substitution can be performed on Br-PMMA to introduce end groups that are not

- (19) Kirby, B. J.; Hasselbrink, E. F., Jr. *Electrophoresis* **2004**, *25*, 187–202.
 (20) Ulman, A. *Chem. Rev.* **1996**, *96*, 1533–1554.
 (21) Wang, J.; Chen, C.; Buck, S. M.; Chen, Z. *J. Phys. Chem. B* **2001**, *105*, 12118–12125.
 (22) Johnson, T. M.; Ross, D.; Gaitan, M.; Locascio, L. E. *Anal. Chem.* **2001**, *73*, 3656–3661.
 (23) McCarley, R. L.; Vaidya, B.; Wei, S.; Smith, A. F.; Patel, A. B.; Feng, J.; Murphy, M. C.; Soper, S. A. *J. Am. Chem. Soc.* **2005**, *127*, 842–843.
 (24) Cheng, J.-Y.; Wei, C.-W.; Hsu, K.-H.; Young, T.-H. *Sens. Actuators, B* **2004**, *99*, 186–196.
 (25) Henry, A. C.; Tutt, T. J.; Galloway, M.; Davidson, Y. Y.; McWhorter, C. S.; Soper, S. A.; McCarley, R. L. *Anal. Chem.* **2000**, *72*, 5331–5337.
 (26) Johansson, B.-L.; Larsson, A.; Ocklind, A.; Ohrlind, A. *J. Appl. Polym. Sci.* **2002**, *86*, 2618–2625.
 (27) Liu, J.; Pan, T.; Woolley, A. T.; Lee, M. L. *Anal. Chem.* **2004**, *76*, 6948–6955.
 (28) Ponter, A. B.; Jones, W. R., Jr.; Jansen, R. H. *Polym. Eng. Sci.* **1994**, *34*, 1233–1238.
 (29) Steen, M. L.; Hymas, L.; Havey, E. D.; Capps, N. E.; Castner, D. G.; Fisher, E. R. *J. Membr. Sci.* **2001**, *188*, 97–114.
 (30) Steen, M. L.; Butoi, C. I.; Fisher, E. R. *Langmuir* **2001**, *17*, 8156–8166.
 (31) Steen, M. L.; Jordan, A. C.; Fisher, E. R. *J. Membr. Sci.* **2002**, *204*, 341–357.
 (32) Lee, J. H.; Park, J. W.; Lee, H. B. *Biomaterials* **1991**, *12*, 443–448.
 (33) Weikart, C. M.; Yasuda, H. K. *J. Polym. Sci., Polym. Chem. Ed.* **2000**, *38*, 3028–3042.
 (34) Goldblatt, R. D.; Ferreiro, I. M.; Nunes, S. L.; Thomas, R. R.; Chou, N. J.; Buchwalter, L. P.; Heidenreich, J. E.; Chao, T. H. *J. Appl. Polym. Sci.* **1992**, *46*, 2189–2202.
 (35) Schroder, K.; Meyer-Plath, A.; Keller, D.; Besch, W.; Babucke, G.; Ohl, A. *Contrib. Plasma Phys.* **2001**, *41*, 562–572.
 (36) Groning, P.; Collaud, M.; Dietler, G.; Schlapbach, L. *J. Appl. Phys.* **1994**, *76*, 887–892.
 (37) Chai, J.; Lu, F.; Li, B.; Kwok, D. Y. *Langmuir* **2004**, *20*, 10919–10927.

- (38) Uyama, Y.; Kato, K.; Ikada, Y. *Adv. Polym. Sci.* **1998**, *137*, 1–39.
 (39) Zangmeister, R. A.; Tarlov, M. J. *Langmuir* **2003**, *19*, 6901–6904.
 (40) (a) Clark, D. T.; Dilks, A. *J. Polym. Sci., Polym. Chem. Ed.* **1977**, *15*, 2321–2345. (b) Grant, J. L.; Dunn, D. S.; McClure, D. J. *J. Vac. Sci. Technol. A* **1988**, *6*, 2213–2220.
 (41) Medard, N.; Soutif, J.-C.; Poncin-Epaillard, F. *Langmuir* **2002**, *18*, 2246–2253.
 (42) Vargo, T. G.; Gardella, J. A., Jr.; Salvati, L., Jr. *J. Polym. Sci., Polym. Chem.* **1989**, *27*, 1267–1286.
 (43) Fritz, J. L.; Owen, M. J. *J. Adhesion* **1995**, *54*, 33–45.
 (44) Schulz, U.; Munzert, P.; Kaiser, N. *Surf. Coat. Technol.* **2001**, *142–144*, 507–511.

compatible with the trichlorosilane treatment and to illustrate the robustness of the modified surfaces. These substitution reactions are not discussed in this paper, as the goal of this paper is to demonstrate the use of water-vapor plasma to activate PMMA surfaces toward reactions with trichlorosilanes.

Experimental Section

Materials. PMMA sheets (CQ Grade, 1.0 mm thick) were purchased from Goodfellow (Devon, PA), sliced into 10 mm \times 10 mm squares, cleaned with petroleum ether and 2-propanol, and degassed at 80 °C overnight in a vacuum oven (150 mTorr) before use. Octadecyltrichlorosilane (OTS, Aldrich Chemical; Milwaukee, WI) and 11-bromoundecyltrichlorosilane (Gelest, Inc.; Morrisville, PA) were used as received. Cyclohexane was distilled from CaH₂ and stored under nitrogen prior to use. Karl Fisher titration indicated cyclohexane water content of approximately 3 ppm.

Plasma Treatment. PMMA samples were exposed to a RF-generated water-vapor plasma (600 mTorr) generated within a March Plasmod GCM-200 (Concord, CA). The reaction chamber was pumped down to less than 200 mTorr prior to the introduction of water vapor. Water vapor was pulled from a degassed water (Millipore, 18 M Ω) source which was cooled to less than 5 °C with external cooling using a water-ice bath for at least half an hour prior to use. Samples were exposed at the appropriate power and time conditions as indicated in the text. Samples were used within an hour of removal from the plasma to minimize hydrophobic recovery.

Silane Treatment. Water-vapor plasma treated PMMA (PT-PMMA) samples were soaked in a 1% v/v cyclohexane (3 ppm H₂O, Karl Fisher titration) solution of the appropriate silane for the length of time as indicated in the text. A continuously nitrogen-purged glovebag was used to maintain a relative humidity of less than 5%, verified using a Omega RH82 handheld humidity meter. After silane treatment, the samples were thoroughly rinsed with petroleum ether, annealed at 70 °C for 1 h in a vacuum oven (150 mTorr), rinsed with methanol, and then dried again in the vacuum oven for at least 2 h. Samples were stored in a desiccator until further experiments.

Contact Angle. Contact angles were measured on a Rame-Hart (Mountain Lake, NJ) XRL C. A. goniometer (Model 100-00) and were measured as the advancing angle of a sessile drop of distilled (Millipore, 18 M Ω) water. Each sample was measured at three to five separate locations on the deposited organic film to check for uniformity. Reported values are an average of these measurements with the associated standard deviation.

XPS. XPS spectra were recorded for surface-functionalized PMMA by a Kratos Axis ULTRA X-ray spectrometer (Al K α radiation, 15 kV, 225 W). Measurements on PMMA substrates were done at pass energies of 160 eV for the survey scans. The detail scans were performed at pass energies of 40 eV with a beam spot size of 0.2 mm. The base pressure for all PMMA measurements was ca. 5×10^{-8} Torr or better vacuum. PMMA samples were attached to the sample holder with UHV-compatible copper (Cu) tape. Different peaks in the spectra can be resolved to about 1 eV. This window is somewhat larger than the instrument limit of 0.3 eV, which can be expected for dielectric substrates due to surface charging.

FTIR-ATR. Spectra were collected on a Nicolet Magna-IR 750 spectrometer (Madison, WI) with a Harrick (Ossining, NY) Seagull reflectance accessory by placing the sample in intimate contact with a Ge hemisphere ($n = 4.0$). For PMMA samples, the incidence and reflection angle was 45°.

Preparation of Microchannels. Microfluidic devices (Figure 1) were made by etching into commercial PMMA sheets (1 mm thick, cut into 25 \times 50 mm pieces) with an oxygen/Argon plasma (150 W, 70 min) with a Si shadow mask to yield 30 mm long 100 \pm 10 μ m wide and 15 \pm 2 μ m deep as measured via profilometry (Tencor P10 profilometer). The total gas pressure during etching was 750 mTorr, and the O₂ flow rate was maintained at 2.5 times that of Ar. These channels connected two reservoirs of 2 mm diameter and approximately the same depth as the channel. Holes (4 mm) were drilled into a cover PMMA sheet to access the reservoirs, and both

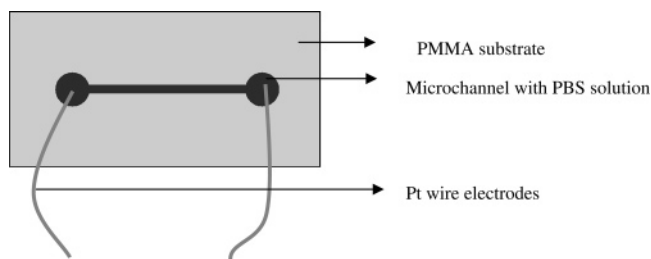


Figure 1. Microfluidic devices were made by etching into commercial PMMA sheets. Each device is 1 mm thick, 25 mm wide, and 50 mm long. Channels are etched into the PMMA with oxygen/argon plasma (150 W, 70 min) with a Si shadow mask to yield 30 mm long channels with cross-sectional dimensions of approximately 15 μ m \times 100 μ m. The reservoirs have the same depth as the channel and are 2 mm in diameter. The microchannel is functionalized and filled with phosphate buffer saline of pH in the range 7.2–7.4.

pieces were annealed in a vacuum oven at 80 °C overnight to remove residual stresses from machining. The pieces were then exposed to the water-vapor plasma and silane solutions. Next, the two pieces were bonded together by contact printing with a commercial adhesive transferred from a PDMS master and thermally bonded at 90 °C with a contact force of 2000 N in an EV501 anodic bonder. Following bonding, the assembled devices were cured for at least 12 h in a vacuum oven at 90 °C to cure the adhesive.

EOF Measurements. EOF characterization was performed on both untreated and surface-modified PMMA devices. The aim of these measurements was to determine the effect, if any, of surface treatments on EOF in comparison to the untreated microchannels. Two devices of each functionalization scheme ($-Br$ or $-CH_3$ termination) were tested. EOF measurements were performed in two steps. For the first step, the reservoirs and the channels were filled with a 10 mM phosphate buffer saline (PBS, Sigma-Aldrich, St. Louis, MO) of pH 7.2–7.4. Pt wires were used as electrodes to establish electrical contact with the PBS in the reservoirs. A current–voltage (I – V) curve was generated to check for electrical continuity and the onset of Joule heating. For all devices tested, the onset of Joule heating was approximately 200–250 V. For the second stage of making actual EOF measurements, one reservoir was replaced with a 5 mM PBS of pH 7.2–7.4 and current was recorded for the 5 mM buffer moving to the 10 mM side for an applied bias of 100 V across the channel with respect to ground. Current was recorded as a function of time as the 5 mM buffer replaced the 10 mM buffer solution in the channel. EOF values were calculated from these measurements by using a current-monitoring method.⁴⁵ In this method, the time taken for current to reach a steady-state or asymptotic value is recorded for a change in buffer concentration in one of the reservoirs. In the present setup, 5 mM PBS replaces the 10 mM PBS.

Before all measurements, the devices were inspected under a microscope to ensure the channels were fully filled and no bubbles were trapped in solution in the channels. Further, the I – V characteristics between the two reservoirs yielded a linear profile indicating electrical continuity.

Results and Discussion

1. Effect of Water-Vapor Plasma Power and Time on Surface Activation. It has been shown previously that PMMA or poly(hydroxyethyl methacrylate) (pHEMA) will adsorb a surface layer of an alkyltrichlorosilane.⁴⁶ However, in the absence of reactive surface functionalization or activation (as is the case for PMMA), any adsorbed silane layer was readily desorbed within 2 h of soaking in methanol. The silane layer on pHEMA was stable under the same conditions, indicating the importance of surface hydroxyls for surface-anchoring reactions with the trichlorosilanes.⁴⁶ To overcome this problem for PMMA, water-

(45) Huang, X.; Gordon, M. J.; Zare, R. N. *Anal. Chem.* **1988**, *60*, 1837–1838.

(46) Khoo, C. G. L.; Lando, J. B.; Ishida, H. *J. Polym. Sci., Polym. Phys. Ed.* **1990**, *28*, 218–232.

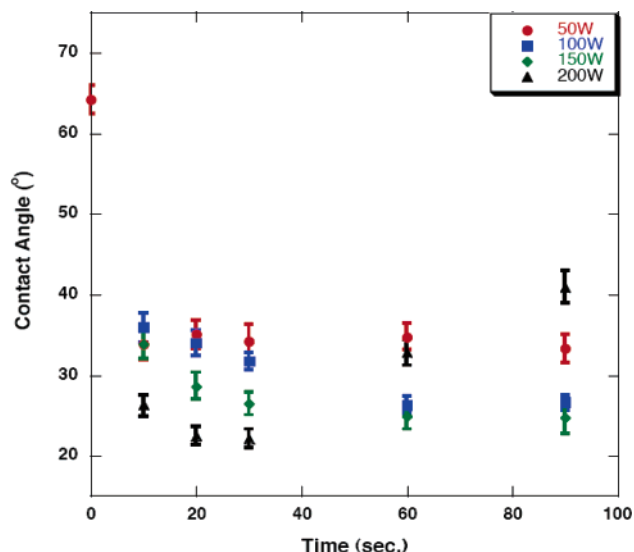


Figure 2. PMMA contact angle as a function of water-vapor plasma power and exposure time.

Table 1. Contact Angle and EOF Data for Functionalized PMMA

surface	contact angle ^d (deg)	lit. (deg, on SiO ₂)	EOF (cm ² /V·s, × 10 ⁻⁴)
bare PMMA	65		2.50 ^c
H ₂ O PT-PMMA	25		
Br-(CH ₂) ₁₁	85	84 ^a	3.43 ± 0.1
CH ₃ (CH ₂) ₁₇ -	104	105–110 ^b	

^a Reference 53. ^b Reference 54. ^c Reference 25. ^d Uncertainty as indicated in text.

vapor plasma was used to activate PMMA surfaces toward reaction with alkyltrichlorosilanes. In the present case, surface activation through water-vapor plasma generates reactive surface functionalities for chemical attachment of surface layers to the PMMA surface.

The effect of water-vapor plasma treatment on the contact angle of PMMA can be seen, as shown in Figure 2. With increasing plasma power, a decrease in the contact angle of the PMMA surface was observed, consistent with increasing hydrophilicity from surface hydroxylation. Increasing the plasma exposure time from 50 to 150 W plasma power leads to a decrease in contact angle for exposures up to 60 s; further increases in exposure time produced insignificant contact angle decreases. At 200 W, sputtering and/or etching of the surface probably begins to dominate and exposure times greater than 30 s yielded films with increasing contact angles, approaching the value for untreated samples. An AFM measurement was conducted for all plasma-treated samples as a function of plasma power (50–200 W at 90 s exposure). The change in surface roughness is within the large uncertainty due to the inherently rough sheets as obtained from the manufacturer, and no measurable change in surface roughness could be ascertained. Thus, the effect of surface roughening due to plasma etching itself on the relative change in wetting properties of the PMMA surface is likely negligible. Plasma exposure conditions of 150 W for 90 s gave a contact angle of 25°, which appeared to be the optimal conditions without any major etching of the sample. This set of conditions was thus chosen for surface activation via hydroxylation.

Hydrophobic recovery of polymer surfaces can also be a factor in the amount of time available for further surface modification.⁴⁷ The effect of plasma power and exposure time on PMMA was examined by the change in contact angle. Initially, after exposure

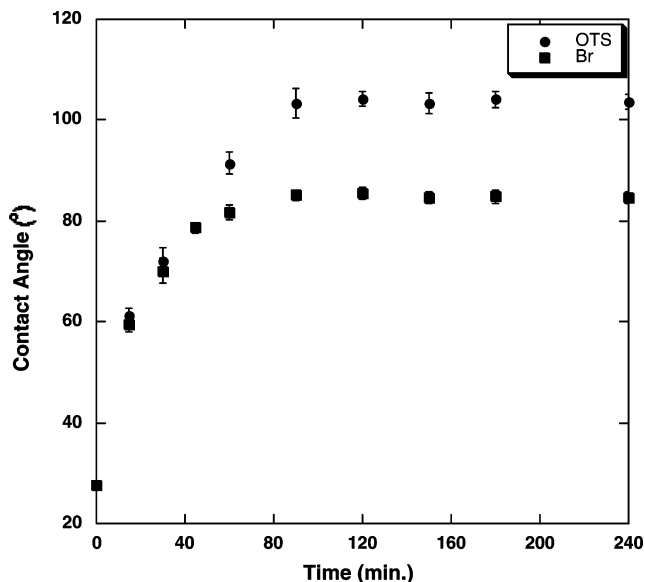


Figure 3. Contact angle measurements for formation of a surface layer of octadecyltrichlorosilane (OTS) and 11-bromoundecyltrichlorosilane on PMMA. Uncertainties reported are standard deviations from average values for multiple measurements.

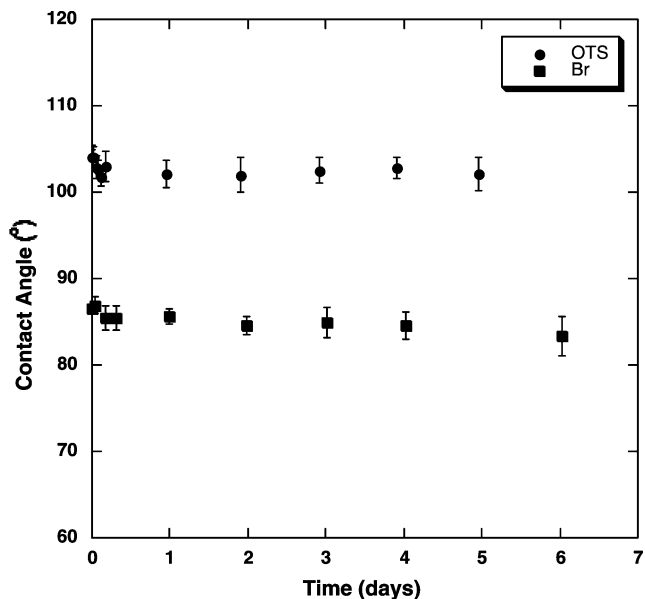


Figure 4. Stability of OTS-PMMA and Br-PMMA toward methanol soaking as measured by changes in contact angle over extended periods of time. Uncertainties reported are standard deviations from average values for multiple measurements.

to the plasma, each sample was stored under water until the contact angle could be measured. This procedure resulted in no correlation between power and time, with all samples scattered about a contact angle of 45° (untreated PMMA,³² 65–70°). The surface after plasma treatment was found to be stable for at least 4 h⁴⁸ before hydrophobic recovery was observed, but all samples were utilized in less than 1 h after plasma exposure.

(47) (a) Chatelier, R. C.; Xie, X.; Gengenbach, T. R.; Griesser, H. J. *Langmuir* **1995**, *11*, 2576–2584. (b) Lim, H.; Lee, Y.; Han, S.; Cho, J.; Kim, K.-J. *J. Vac. Sci. Technol. A* **2001**, *19*, 1490–1496.

(48) Hydrophobic recovery appears to be linked to water exposure. Identically prepared samples displayed differing rates of hydrophobic recovery depending on how often contact angle measurements were made. More frequent measurements (every hour) appear to show a faster rate than when measurements are made over longer time frames (for example, every 8 h). The act of measuring the surface contact angles appears to encourage surface reorganization.

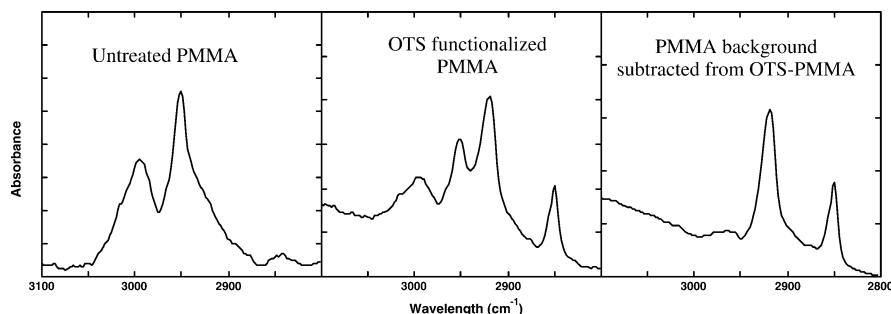


Figure 5. FTIR-ATR spectra of OTS-PMMA. Left to right: untreated PMMA, OTS-PMMA, and OTS-PMMA with PMMA background subtracted. The ordinate shows the absorbance (a.u.), and the abscissa the wavenumber (cm^{-1}).

2. Formation and Characterization of Functional Surface Layers on PT-PMMA. To take advantage of the increased surface reactivity of water-vapor plasma-treated PMMA (PT-PMMA), a reactant was necessary that would react rapidly and irreversibly with the freshly introduced surface hydroxyl moieties. Alkyltrichlorosilanes were chosen for surface modification due to their facile reactivity with free alcohols to form siloxane-based surface layers. While the water-vapor plasma hydroxylation provided attachment points for the surface layer to adhere to the PMMA, an additional benefit of water-vapor plasma exposure is the possible introduction of an adsorbed water layer³⁰ on the surface that has been shown to be essential for the formation of SAMs of alkyltrichlorosilanes on silicon.²⁰

Treatment of PT-PMMA with 1% v/v OTS in cyclohexane leads to the formation of a surface layer, as indicated by the increase in surface contact angle from 25° to 104° (Table 1). Cyclohexane was used for layer depositions since it will not cause surface damage to the PMMA. Toluene, which is commonly used for SiO_2 modification, causes greater surface damage, leading to irreproducibility issues. As shown in Figure 3, surface layer formation was complete in approximately 2 h; longer exposure times had no noticeable effect on the surface contact angle. The samples (OTS-PMMA) were rinsed with copious amounts of petroleum ether and methanol to remove any nonbonded contaminants, as well as islands of hydrogen-bonded silanol aggregates. Samples were then annealed in a vacuum oven at 70°C to encourage complete bond formation between the surface and siloxane layer. Control samples exposed to plasma treatment and then only to solvent did not show changes in contact angle. The same conditions can be used to apply other functional trichlorosilanes to the surface. For example, 11-bromoundecyltrichlorosilane gave a modified surface with a contact angle of 85° (Br-PMMA, Table 1) in 2 h (Figure 3). In both cases, OTS-PMMA and Br-PMMA, contact angles measured were consistent with literature values of similar layers on SiO_2 (Table 1).

3. Characterization of the Surface Functional Layer.

3.1. Stability. Exposure to silane solutions without plasma treatment did allow for formation of an adsorbed layer on the PMMA surface. Any material deposited this way was readily rinsed away with methanol to yield surface contact angles identical to untreated samples. In contrast to surface-adsorbed layers, the surface layer formed through water-vapor plasma followed by silane treatments appears to be bonded to the polymer surface. The surface hydroxylation from the water-vapor plasma yielded hydroxyl groups that are reactive toward the trichlorosilanes in solution. The subsequent surface layers are stable to rinsing after deposition onto PT-PMMA with petroleum ether (to remove nonbonded molecules) and methanol (to remove any hydrogen-bonded silanols, as well as polysilanols). In addition, as shown in Figure 4, both OTS-PMMA and Br-PMMA may be soaked

for extended periods of time in methanol without changes in surface contact angles. Over the course of 5 days of soaking, no evidence of contact angle changes of either the OTS-PMMA or Br-PMMA was observed. The same surfaces are also stable to soaking in water or DMF/water mixtures.⁴⁹

3.2. FTIR-ATR. The introduction of an adherent layer onto PMMA was visualized spectroscopically via p-polarized FTIR-ATR. As is shown in Figure 5, the addition of an OTS layer on PMMA produced a spectrum with an increased absorbance in the C-H stretching region. The signal due to the OTS layer is overlapped by the background spectra of the underlying PMMA due to the relatively deep penetration depth of the incident radiation (a few micrometers compared to a few nanometers for XPS). Subtraction of the background PMMA signal provided a spectrum of the OTS layer as a pair of sharp signals at 2920 and 2850 cm^{-1} (Figure 5). This spectrum matches previous reports for monolayers of OTS on SiO_2 ,⁵⁰ as well as alkyl carboxylic acid monolayers deposited via Langmuir-Blodgett techniques.⁵¹

3.3. XPS. To monitor the elemental composition on introduction of new functionality onto the PMMA surfaces, XPS was utilized to assign elemental compositions to the freshly prepared layers. The takeoff angle for the electron detector was 90° ; however, the penetration depth of the analysis was approximately 10 nm. Peaks were not deconvoluted due to uncertainties introduced (peak shifting and broadening) from sample charging of the nonconductive PMMA. The signals from the new surface modifications were detectable as changes with respect to unmodified PMMA. A blank PMMA control shows only C (1s, $\sim 287\text{ eV}$) and O (1s, $\sim 533\text{ eV}$) as major elemental components. OTS-PMMA showed a pair of peaks at 104 eV characteristic of Si, as well as C (1s, $\sim 287\text{ eV}$) and O (1s, $\sim 533\text{ eV}$). OTS-PMMA indicated carbon enrichment in the surface of the polymer as compared to the untreated PMMA (see Supporting Information).

For Br-PMMA, in addition to new signals at 104 eV for Si (2p), signals clearly assignable to Br (3s), Br (3p), and Br (3d) can be seen in Figure 6. These illustrate the introduction of the Br-undecylsiloxane functionalities on the surface. In addition, the lack of chlorine incorporation in either film indicates the complete hydrolysis of the initial trichlorosilanes.

4. EOF Measurements. Figure 7 shows current versus time data for replacement of 10 mM PBS by 5 mM PBS for an applied voltage of 100 V across the microchannel at a pH of 7.2–7.4. The total channel length is 30 mm. The EOF was found to be $3.43 \times 10^{-4} \pm 1 \times 10^{-5}\text{ cm}^2/\text{V}\cdot\text{s}$ for the -Br functionalized channel. The reported value in the literature²⁵ for a bare PMMA

(49) There were low levels of surface Si contamination of our blanks, as seen by XPS. The surface could potentially be cleaned by washing with DMF/water solutions.

(50) Brunner, H.; Mayer, U.; Hoffmann, H. *Appl. Spec.* **1997**, *51*, 209–217.

(51) Chen, S. H.; Frank, C. W. *Langmuir* **1989**, *5*, 978–987.

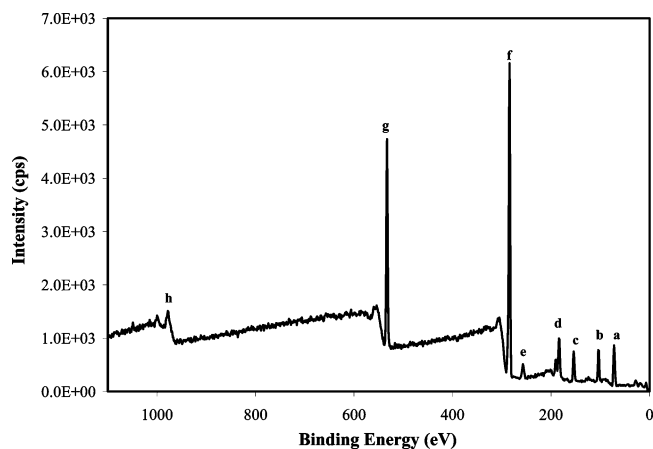


Figure 6. XPS of Br-PMMA. The peaks are shown as indicated. (a) Br (3d), (b) Si (2p), (c) Si (2s), (d) Br (3p), (e) Br (3s), (f) C (1s), (g) O (1s), (h) O (Auger).

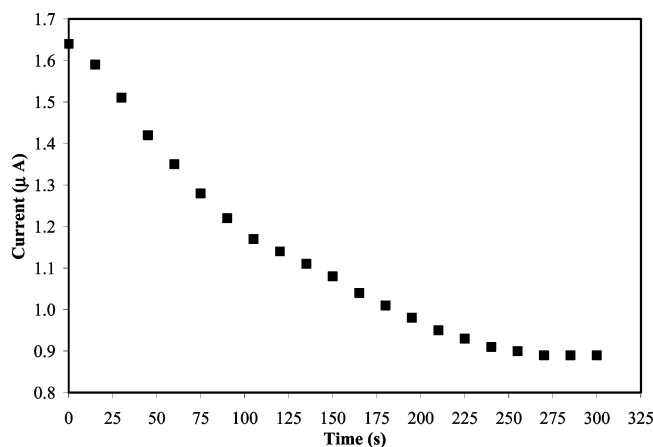


Figure 7. Current measurement as a function of time for replacing 10 mM PBS solutions within Br-PMMA microchannels with 5 mM PBS on application of a 100 V bias across the channel. A schematic for the model test device is shown in Figure 1. Uncertainty in current measurements is on the order of ± 10 nA and in measurement of time ± 1 s.

sample is on the order of $2.5 \times 10^{-4} \text{ cm}^2/\text{V}\cdot\text{s}$ (Table 1). The EOF value for untreated PMMA is reported for a pH of 7 for a low buffer concentration of 10 mM and a high buffer concentration of 100 mM with an applied electric field strength of 150 V/cm.

The difference in measured EOF in comparison to the untreated PMMA is attributed to the 11-bromoundecyltrichlorosilane layer.

The $-\text{CH}_3$ channel could not be successfully filled with the aqueous PBS due to the highly hydrophobic nature of the functionalized channel (contact angle $\approx 104^\circ$). The channel could only be partially filled with air bubbles trapped in the channel. No EOF values were obtained for these devices.

Conclusions

The efficacy of water-vapor plasma for the activation of PMMA surfaces for subsequent reaction with trichlorosilanes to change surface functionalities and energies has been demonstrated in this paper. Surface characterization done using multiple techniques indicates that these layers are uniform and stable upon storage under ambient conditions for extended periods of time without evidence of surface deterioration. Nucleophilic substitution on Br-terminated surface layers can allow access to surface functionalities that are not compatible with the trichlorosilane deposition process.⁵² This methodology can enable placement of functional layers onto PMMA surfaces. In turn, these polymer layers may be integrated into working MEMS devices to affect device operations.

Acknowledgment. The authors thank the National Science Foundation for financial support for the current research through the Center for Nano-Chemical-Electrical-Mechanical Manufacturing Systems (Nano-CEMMS) under DMI-0328162 and the Science and Technology Center of Advanced Materials for the Purification of Water with Systems (WaterCAMPWS) under Agreement No. CTS-0120978. XPS and SIMS were carried out in the Center for Microanalysis of Materials, University of Illinois, which is partially supported by the U.S. Department of Energy under Grant No. DEFG02-91-ER45439. We thank Rick Haasch and Jinju Lee for their assistance in obtaining XPS and SIMS data, respectively. We also thank Jamie Iannacone and Bruce Flachsbart for their assistance with EOF measurements.

Supporting Information Available: XPS data for all surface functionalization not shown in the text and ToF-SIMS data for Br-PMMA. This material is available free of charge via the Internet at <http://pubs.acs.org>.

LA052977T

(52) Baker, M. V.; Watling, J. D. *Langmuir* **1997**, *13*, 2027–2032.

(53) Wasserman, S. R.; Tao, Y.-T.; Whitesides, G. M. *Langmuir* **1989**, *5*, 1074–1087.

(54) Kumar, N.; Maldarelli, C.; Steiner, C.; Couzis, A. *Langmuir* **2001**, *17*, 7789–7797.